PU/NE-01-3

U. S. Department of Energy
Nuclear Engineering Education Research

ANALYTICAL AND EXPERIMENTAL STUDY OF THE EFFECTS OF NON-CONDENSABLE IN A PASSIVE CONDENSER SYSTEM FOR THE ADVANCED BOILING WATER REACTOR

Yearly Report
(May, 2000 to April, 2001)

S. T. Revankar and D. Pollock

PURDUE UNIVERSITY
SCHOOL OF NUCLEAR ENGINEERING

U. S. Department of Energy
Nuclear Engineering Education Research

ANALYTICAL AND EXPERIMENTAL STUDY OF THE EFFECTS OF NON-CONDENSABLE IN A PASSIVE CONDENSER SYSTEM FOR THE ADVANCED BOILING WATER REACTOR

Yearly Progress Report
May, 2000 to April, 2001

Contact: Dr. Shripad T. Revankar
School of Nuclear Engineering
Purdue University
West Lafayette, In 47907-1290

765-496-1782
shripad@ecn.purdue.edu

Contributing Authors:

S. T. Revankar*, and D. Pollock

Purdue University
School of Nuclear Engineering
West Lafayette, IN 47906-1290

May 2001

* *Project Director*

CONTENTS

LIST OF FIGURES

LIST OF TABLES

ACRONYMS

ABWR	Advanced Boiling Water Reactor
AP600	Advanced Passive 600 MWe Pressurized Reactor
DOE	Department Of Energy
DW	Dry Well
GDCS	Gravity Drain Cooling System
GE	General Electric
GE-SBWR	600 Mwe GE designed Simplified Boiling Water Reactor
ICS	Isolation Condensation System
LOCA	Loss Of Coolant Accident
LWR	Light Water Reactor
MIT	Massachusetts Institute of Technology
NRC	Nuclear Regulatory Commission
RELAP5	A Reactor Safety Analysis Code
RPV	Reactor Pressure Vessel
SBWR	Simplified Boiling Water Reactor
SBWR-600	600 MWe GE Designed Simplified Boiling Water Reactor
SP	Suppression Pool
UCB	University of California Berkeley

NOMENCLATURE

c_o	Concentration of noncondensable
c_p	Specific heat [j/kg·C]
d,D	Diameter [m]
f	Friction factor
Gr	Grashof number Eq. (215)
g	Gravitational acceleration [m/s^2]
H	Height [m]
h	Heat transfer coefficient[W/m^2·C]
i	Enthalpy [J/kg]
i_{fg}	Latent heat of vaporization [J/kg]
Ja	Jakob number Eq.
k	Conductivity [W/m^2·C]
$\dot{m}$	Mass flow rate [kg/s]
n, N	Number
Pr	Prandtl number Eq.
q''	Heat flux [W/m^2]
$\dot{Q}_c$	Condensation power
R	Universal gas constant [kJ/kg·mol-K]
Re	Reynold's number
t	Time [s]
T	Temperature [K]
U	Overall heat transfer coefficient [W/m^2·C]
v,V	Volume [m^3]
W_a	Noncondensable mass fraction

Greek Symbols

α_s	Thermal diffusivity [m^2/s]
β	Volumetric thermal expansion coefficient [K^{-1}]
μ	Dynamic viscosity [kg/m·s]
ν	Kinematic viscosity [m^2/s]
ρ	Density [kg/m^3]

Subscripts

a	Ambient, air
b	Bulk
cond	Condensation
DW	Drywell
f	Liquid
g	Gas
i	ith component

m	Model
o	Reference point/component
p	Prototype
pccs	PCCS
R	Ratio
SP	Suppression Pool
T	Pool water

EXECUTIVE SUMMARY

The main goals of this three-year research project are to: 1) obtain experimental data on the phenomenon of condensation of steam in a vertical tube in the presence of non-condensable for flow conditions of PCCS, 2) develop a analytical model for the condensation phenomena in the presence of non-condensable gas for the vertical tube, and 3) assess the RELAP5 computer code against the experimental data.

The project involves experimentation, theoretical modeling and a thermalhydraulic code assessment. It involves graduate students and undergraduate students participations providing them with exposure and training in advanced reactor concepts and safety systems.

The present 3-year research program is structured around six tasks. Task 1 is to design a well-scaled condensation test facility and identify PCCS condenser flow conditions based on scaling. Task 2 is to obtain database on local and overall condensation heat transfer coefficient as a function of flow condition and inlet non-condensable gas concentration. Task 3 is to develop an analytical model for condensation in the vertical tube in the presence of non-condensable gas for PCCS flow conditions. Task 4 is to develop correlation for heat transfer coefficient for condensation in the presence of con-condensable gas based on the experiments and analytical model. Task 5 is to assess RELAP5 code against the experimental data. This report documents the first phase of the program and progress achieved from May 2000 to April 2001 in these tasks.

Task 1 on the scaling analysis and the design of the test facility has progressed as planned. On Task 3 initial analytical model for the condensation in the vertical tube in the presence of non-condensable gas for forced flow condition is completed. An extension of four month time was requested with DOE for completion of first year part of the Task 2.

1. INTRODUCTION

1.1 Significance of the Problem

The condensation phenomenon plays an important role in the heat transfer process in many industrial applications. The condensation mode of heat transfer is often used in engineering because of high heat transfer coefficients. However, the presence of the noncondensable gases in vapors can greatly inhibit the condensation process. Noncondensable gas unable to pass into the condensate film, accumulates at the liquid-vapor interface leading to a decrease in vapor partial pressure and thus the interface temperature at which condensation occurs. In the nuclear reactor industry, condensation heat transfer is very important in many situations. In the case of loss of coolant accident (LOCA), a large portion of the heat is removed by condensation of steam in the steam generators in reflux condensation mode. The presence of the noncondensable hampers the heat removal process.

In the advanced light water reactors such as the Westinghouse designed Advanced Passive 600 MWe (AP600) [1.1] and General Electric Simplified Boiling Water Reactor (SBWR) [1.2], there is a greater emphasis on replacing the active systems with passive systems in order to improve the reliability of operation. For example, the SBWR is based on natural circulation cooling. SBWR uses the gravity driven cooling system (GDCS) as an emergency core cooling system following an accident. After the reactor is scrammed the pressure vessel is depressurized with system of valves and thus pressure in the vessel is reduced so that the GDCS is made functional. The containment steam is condensed by a condenser system called Passive Containment Cooling System (PCCS). In this reactor the containment pressurization thus depends on the condensing capability of the PCCS after the blowdown process. Development programs on advanced light water reactor based on passive safety systems are underway in Europe and Japan. Design development of the European Simplified Boiling water Reactor (ESBWR) [1.3] and Japanese SBWR [1.4] are the longer-term goals in this effort.

In the SBWR the PCCS is a passive heat exchanger that allows the transfer of heat via steam condensation to the water pool. The PCCS condenser must be able to remove sufficient energy from the reactor containment to prevent containment from exceeding its design pressure following a design-basis accident. The efficient performance of the PCCS condenser is thus

vital to the safety of the SBWR. The rate of heat transfer in the PCCS condenser is strongly coupled to the hydrodynamic characteristics of the PCCS. Hence a detailed knowledge of the variation of local heat transfer coefficient is necessary in order to predict the performance of the PCCS and for design optimization.

Uchida et al's [1.5] experiments on steam-gas condensation on outside wall of vertical tube provided first practical correlation for the degradation of condensation. Since then several theoretical works on the effects of the non-condensable on condensation in vertical pipe have been conducted [1.6-1.8]. The relevant separate effects experiments on PCCS condensation under the presence of noncondensable gas were conducted at Massachusetts Institute of Technology (MIT) [1.9,1.10] and at University of California Berkeley (UCB) [1.11,1.12]. Both MIT and UCB tests provided a new database and correlation for forced convection condensation of steam in a vertical tube in the presence of noncondensable gas. The flow of steam/gas mixture in the PCCS condenser tube as discussed in following section 1.2 is not always forced convection. Hence the UCB and MIT correlations do not apply for all flow conditions in the PCCS. This research addresses this particular problem by perform careful experiments for the flow conditions expected in the PCCS condenser and develop analytical model to predict the condensation heat transfer characteristics of PCCS in the presence of non-condensable gas. In addition to this task a RELAP5 code model will be developed for PCCS condensation in the presence of non-condensable and the RELAP5 code assessment is performed.

1.2 PCCS Operation

In order to model the condensation in PCCS, it is important to study the operation of the PCCS and identify the flow conditions in the PCCS. A flow diagram of the PCCS is shown in Figure 1. The PCCS condensers condense steam from the drywell (DW). They are immersed in a large interconnected Isolation Condenser System (ICS) pool of water. The ICS pool is located outside and above the containment. Condensed water produced in the PCCS condensers returns to the GDCS pool and then to the Reactor Pressure Vessel (RPV). Non-condensable gases from the PCCS are vented to the Suppression Pool (SP). The driving head of the PCCS is provided by the pressure difference between the DW and the SP. There are no valves or pumps in the

PCCS and any operational actions or signals are not needed which makes the PCCS a truly passive system.

Three different operational modes are possible in the PCCS depending on the non-condensable gas concentration and the pressure difference between the DW and the SP. These are Bypass Mode, Continuous Condensation Mode and Cyclic Condensation and Venting Mode. The PCCS will be in Bypass Mode when the pressure difference between the DW and the SP is relatively high compared with the head due to the submergence of the vent line in the SP. This condition is realized during the blowdown process. In this mode, steam and non-condensable gas pass through the PCCS condensers with condensation. This mode of operation corresponds to forced convection. When the pressure difference between the DW and the SP is comparable with the head due to the submergence of the vent line in the SP, the PCCS will be in either Continuous Condensation mode or Cyclic Condensation and Venting Mode depending on the non-condensable gas concentration. The PCCS will be in Continuous Condensation Mode when the non-condensable gas concentration is very low. This condition will be obtained in the later stage of an accidental transient after most of non-condensable gas is vented to the SP.

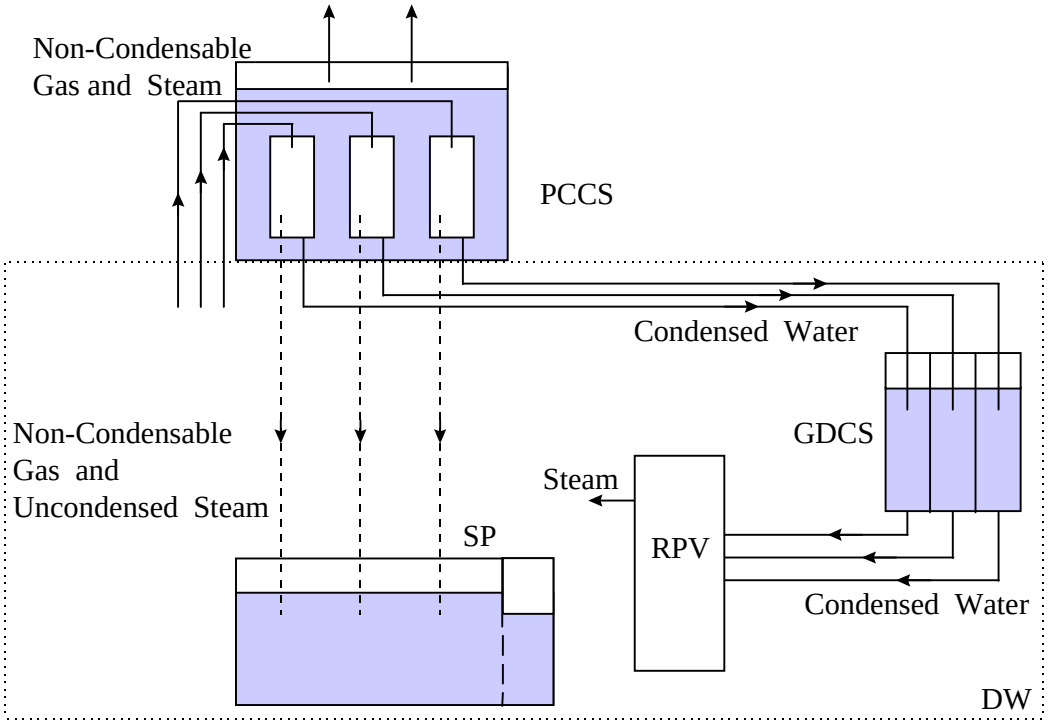

Figure 1.1. Flow diagram in SBWR during a loss of coolant accident

The PCCS will be in Cyclic Condensation and Venting Mode when the non-condensable gas concentration is relatively high. This condition sets in immediately after the blow down process. In this mode, steam has enough time to be condensed in the PCCS condensers. In the condensation process, non-condensable gas is accumulated in the PCCS condensers. Hence the DW pressure begins to rise as the condensation decreases. The DW pressure continues to increase after the condensation process totally stops. When the pressure difference is high enough to overcome the head due to submergence of the vent line in the SP, non-condensable gas is vented to the SP. The condensation process begins again after clearing of non-condensable gas from the PCCS. This cycle repeats. Thus the forced convection flow condensation is one of three PCCS flow conditions.

1.3 References

1.1. Bruschi H J., AP600-safety through simplicity. [Conference Paper] Proceedings of the International Topical Meeting on Advanced Reactors Safety. ANS. Part vol.1, pp.3-8 vol.1. La Grange Park, IL, USA, (1997).

1.2. GE Nuclear Energy, SBWR Standard Safety Analysis Report, Report No. 25A5113 Rev. A, August, (1992).

1.3. Bandurski T. Dreier J. Huggenberger M. Aubert C. Fischer O. Healzer J. Lomperski S. Strassberger H-J. Varadi G. Yadigaroglu G. PANDA passive decay heat removal transient test results. Eighth International Topical Meeting on Nuclear Reactor Thermal-Hydraulics. NURETH-8. New Horizons in Nuclear Reactor Thermal-Hydraulics. Atomic Energy Soc. Japan. Part vol.1, pp.474-84 vol.1. Tokyo, Japan, (1997).

1.4. Yoshioka Y. Arai K. The analysis of PCCS heat removal performance for the 1300 MWe simplified BWR.Eighth International Topical Meeting on Nuclear Reactor Thermal-Hydraulics. NURETH-8. New Horizons in Nuclear Reactor Thermal-Hydraulics. Atomic Energy Soc. Japan. Part vol.1, pp.468-73 vol.1. Tokyo, Japan (1997).

1.5. Uchida, H., Oyama, A., and Togo, Y., Evaluation of Post-Incident Cooling Systems of Light Water Reactors, Proc. 3rd Int. Conf. Peaceful Uses of Atomic Energy, Vienna, Austria, Vol. 13, p. 93, International Atomic Energy Agency (1964).

1.6. Wang, D. Y. and Tu, C. J., Effects of Noncondensable Gas on Laminar Film Condensation in a Vertical Tube, Int. J. Heat Mass Transfer, Vol. 31, 2339 (1988).

1.7. Denny, V. E., Mills, A. F. and Jusionis, V. J., Laminar Film Condensation from a Steam-Air Mixture Undergoing Forced Flow Down a Vertical Surface, J. Heat Transfer, Vol. 93, 297 (1971)

1.8. Al-Diwani, H. K. and Rose, J. W., Free Convection Film Condensation of Steam in the Presence of Noncondensing Gases, Int. J. Heat Mass Transfer, Vol. 16, 1359 (1973).

1.9. Siddique, M., The Effects of Noncondensable Gases on Steam Condensation under Forced Convection Conditions, Ph.D. Dissertation, Massachusetts Institute of Technology (1992).

1.10. Siddique, M., Golay, M. W., and Kazimi, M. S., Local Heat Transfer Coefficients for Forced Convection Condensation of Steam in a Vertical Tube in the Presence of a Noncondensable Gas, Nucl. Technol., Vol. 102, 386 (1993).

1.11. Vierow, K. M., Behavior of Steam-Air Systems Condensing in Concurrent Vertical Downflow, MS Thesis, Department of Nuclear Engineering, University of California at Berkeley (1990).

1.12. Ogg D. G., Vertical Downflow Condensation Heat Transfer in Gas-Steam Mixture, MS Thesis, Department of Nuclear Engineering, University of California at Berkeley (1991)

2. OBJECTIVES

The goals of this research are to: 1) obtain experimental data on the phenomenon of condensation of steam in a vertical tube in the presence of non-condensable for flow conditions of PCCS, 2) develop a analytical model for the condensation phenomena in the presence of non-condensable gas for the vertical tube, and 3) assess the RELAP5 computer code against the experimental data.

The objectives of the research are:

1. Design a well-scaled condensation test facility and identify PCCS condenser flow conditions based on scaling.
2. Obtain database on local and overall condensation heat transfer coefficient as a function of flow condition and inlet non-condensable gas concentration.
3. Develop an analytical model for condensation in the vertical tube in the presence of non-condensable gas for PCCS flow conditions.
4. Compare analytical predictions and experimental data on heat transfer coefficient.
5. Develop a correlation for heat transfer coefficient for condensation in the presence of non-condensable for use in codes.
6. Assess RELAP5 code against the experimental data.

3. FIRST PHASE MILE STONE AND TECHNICAL TASKS

Here the milestones for the first phase of the project are presented. The first phase of the project is performed during the first year period. These milestones are listed below along with their respective technical tasks.

- PCCS scaling analysis: Technical task under this milestone is to perform scaling analysis for PCCS condenser design.
- Experimental program for 5.04 cm condenser tube: Under this milestone the technical tasks are to design a 5.04 cm condenser tube with adequate instrumentation, construct an experimental facility and perform testing.
- Experimental data on 5.04 cm condenser tube: Under this milestone the technical tasks are to obtain experimental data on heat transfer for 5.04mm condenser for three PCCS flow conditions: forced flow; continuous condensation (with zero flow velocity at bottom of the condenser); and cyclic condensation.

4. SCALING ANALYSIS

The objective of this task was to develop a scaling methodology that is used in the design of the condenser, analysis of the data from the scaled facility, scale-up of the data from scaled model to the prototype design. In this chapter a scaling analysis is presented. The scaling analysis identifies key thermalhydraulics parameters that govern condensation in the PCCS.

4.1 PCCS Heat Transfer

The PCCS condensers provide decay heat removal by condensing steam from the drywell and supplying condensate water to the RPV through the GDCS tanks. The scaling of the heat transfer rate through the condenser is given by

$$\dot{Q}_{pccs} = N_{tubes}\ N_{units}\, U\, A_i \left(T_g - T_p\right), \tag{4.1}$$

where N_{tubes} is the number of PCCS condenser tubes, N_{units} is the number of PCCS units, U is the overall heat transfer coefficient, A_i is the inner surface area of a condenser tube, and T_g and T_p are the steam and PCCS pool temperatures, respectively (see Figure 4.1). The overall heat transfer coefficient is given by

$$U = \left[\frac{1}{h_c} + \frac{1n\left(D_o / D_i\right) D_i}{2\,k_w} + \frac{D_i}{h_p\, D_o}\right]^{-1}. \tag{4.2}$$

In the RHS of Eq. (4.2), the first term corresponds to the tube side condensation heat transfer coefficient, the second term corresponds to the tube wall conduction heat transfer coefficient, and the third term corresponds to the outside tube pool heat transfer coefficient.

The condensation heat transfer coefficient is for the condensation of steam and air or nitrogen mixture in a vertical tube. Siddique et al. [4.1] have studied the condensation heat transfer coefficient for steam-air mixture in the tube. The condensation heat transfer Nusselt number given by them is

$$Nu_c = \frac{h_c\, D_i}{k_g} = 6.213\, Re^{0.223} \left(\frac{W_{a,w} - W_{a,b}}{W_{a,b}}\right)^{1.44} Ja^{-1.253}, \tag{4.3}$$

where

$$Ja = \frac{c_p \left(T_b - T_w\right)}{i_{fg}} \qquad \text{(Jakob number)} \tag{4.4}$$

$$\mathrm{Re} = \frac{\rho_m u_m D_i}{\mu_m} \qquad \text{(Reynolds number)} \qquad (4.5)$$

$$W_a = \frac{\dot{m}_a}{\dot{m}_a + \dot{m}_v} \quad . \qquad (4.6)$$

The poolside heat transfer coefficient, h_p, depends on whether poolside transfer is due to boiling or natural convection.

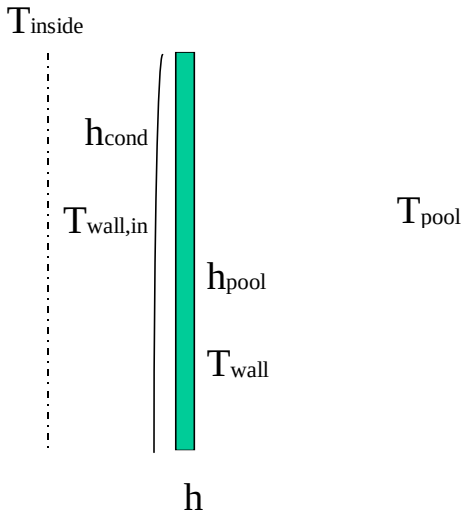

Figure 4.1 PCCS Tube Condensation

For natural convection, the heat transfer Nusselt number is given by

$$\mathrm{Nu}_p = \frac{h_p L_{tube}}{k_p} = 0.021\left(\mathrm{Gr}\ \mathrm{Pr}\right)^{0.4}, \qquad (4.7)$$

where

$$\mathrm{Gr} = \frac{g\beta\left(T_w - T_p\right)L_{tube}^3}{\nu^2} \qquad \text{(Grashof number)} \qquad (4.8)$$

$$\mathrm{Pr} = \frac{\nu}{\alpha} \qquad \text{(Prandtl number)} \; . \qquad (4.9)$$

For the correct scaling of heat removal by the PCCS condensers we should have

$$\frac{\left(\dot{Q}_{pccs}/(\dot{m}i_{fg})\right)_m}{\left(\dot{Q}_{pccs}/(\dot{m}i_{fg})\right)_p}=1, \tag{4.10}$$

where $\dot{m}$ is the inlet steam mass flow rate to the PCCS condenser. From Eqs. (4.1) and (4.10), the scaling requirement for PCCS condenser heat removal rate is given as

$$\left(N_{tubes}\,N_{units}\,U\,A_i\left(T_b-T_p\right)/(\dot{m}i_{fg})\right)_R=1 \tag{4.11}$$

If the prototype and model have the same operating pressure condition and use the same operating fluid (water), then the temperature difference can be preserved. From Eqs. (4.10) and (4.11) we obtain,

$$\frac{\left(\dot{Q}_{pccs}/(\dot{m}i_{fg})\right)_m}{\left(\dot{Q}_{pccs}/(\dot{m}i_{fg})\right)_p}=$$

$$\left(\frac{N_m}{N_p}\right)_{tubes}\left(\frac{N_m}{N_p}\right)_{units}\left(\frac{U_m}{U_p}\right)\left(\frac{A_m}{A_p}\right)_i\left\{\frac{\left(T_b-T_p\right)_m}{\left(T_b-T_p\right)_p}\right\}\left(\frac{\dot{m}_p}{\dot{m}_m}\right)\left[\frac{\left(i_{fg}\right)_p}{\left(i_{fg}\right)_m}\right] \tag{4.12}$$

Equation (4.12) is used in the design of the PCCS condenser.

First, we evaluate $\left(\frac{U_m}{U_p}\right)$ or $(U)_R$.

4.2 Scaled System

Calculations were performed for scaling the prototype PCCS condenser. The prototype system is General Electric 600 MWe Simplified Boiling Water Reactor PCCS. Its relevant dimensions are given in Table 4.1 [4.2]. The scaling criteria for the flow in thermalhydraulic system are available [4.3]. These scaling criteria were used in the design of the condenser. Various scaled sizes were considered for calculations. The height scaling was taken as ¼ and ½. The volume scaling used was 1/400, 1/600, 1/800, 1/1000 and 1/1600. In Table 4.2 the ratio of various condenser parameters are shown for different volume and height scaling. This table is used in selecting the condenser tube diameter, height, flow rates and the power levels. For ½ height scaling, 1/1 tube diameter scaling and 1/400 volume scaling, the velocity ratio or Reynolds number ratio is 0.71. Thus the model requires lower flow velocity. In the case of ¼ height scaled condenser the model requires velocity ratio of 0.5.

Table 4.1 PCCS Condenser in GE SBWR-600

No. of Condenser units	3
Modules per unit	2
Tubes per module	248
Total heat transfer area (m2):	Tube Inside=400, Tube Outside=427.5
Total flow area (m2)	2.6
Number of Tubes	496
Condenser tubes:	Length (mm)= 1800, O.D. (mm)=50.8, I.D. (mm)+47.5
Material	SS/Inconel
Headers per module:	I.D. (mm)= 660, Volume (m3)= 0.78
Header center to IC pool bottom (mm)	670

Table 4.2 Condenser Scaling

Scaling Volume, Height	**D_R†**	**V_R**	**H_R**	**A_R**	**P_R, HTA_R**	**FLA_R**	**H Mm**	**Tube #**	**P_T KW (at 2%)**	**v_R**	**Re_R**	**P_T kW (at 0.4%)**
1/400, 1/4	1	0.0025	0.25	0.0100	0.0050	0.0200	450	9.92	20.161	0.50	0.50	4.03
1/600,1/4	1	0.0017	0.25	0.0067	0.0033	0.0133	450	6.61	20.161	0.50	0.50	4.03
1/800,1/4	1	0.0013	0.25	0.0050	0.0025	0.0100	450	4.96	20.161	0.50	0.50	4.03
1/1000, 1/4	1	0.0010	0.25	0.0040	0.0020	0.0080	450	3.97	20.161	0.50	0.50	4.03
1/1200, 1/4	1	0.0008	0.25	0.0033	0.0017	0.0067	450	3.31	20.161	0.50	0.50	4.03
1/1600,1/4	1	0.0006	0.25	0.0025	0.0013	0.0050	450	2.48	20.161	0.50	0.50	4.03
1/400, 1/2	1	0.0025	0.5	0.0050	0.0035	0.0071	900	3.51	40.323	0.71	0.71	8.06
1/600,1/2	1	0.0017	0.5	0.0033	0.0024	0.0047	900	2.34	40.323	0.71	0.71	8.06
1/800,1/2	1	0.0013	0.5	0.0025	0.0018	0.0035	900	1.75	40.323	0.71	0.71	8.06
1/1000, 1/2	1	0.0010	0.5	0.0020	0.0014	0.0028	900	1.4	40.323	0.71	0.71	8.06
1/1200, 1/2	1	0.0008	0.5	0.0017	0.0012	0.0024	900	1.17	40.323	0.71	0.71	8.06
1/1600,1/2	1	0.0006	0.5	0.0013	0.0009	0.0018	900	0.88	40.323	0.71	0.71	8.06
1/400, 1/4	0.5	0.0025	0.25	0.0100	0.0050	0.0100	450	19.8	10.081	0.50	0.25	2.02
1/600,1/4	0.5	0.0017	0.25	0.0067	0.0033	0.0067	450	13.2	10.081	0.50	0.25	2.02
1/800,1/4	0.5	0.0013	0.25	0.0050	0.0025	0.0050	450	9.92	10.081	0.50	0.25	2.02
1/1000, 1/4	0.5	0.0010	0.25	0.0040	0.0020	0.0040	450	7.94	10.081	0.50	0.25	2.02
1/1200, 1/4	0.5	0.0008	0.25	0.0033	0.0017	0.0033	450	6.61	10.081	0.50	0.25	2.02
1/1600,1/4	0.5	0.0006	0.25	0.0025	0.0013	0.0025	450	4.96	10.081	0.50	0.25	2.02
1/400, 1/2	0.5	0.0025	0.5	0.0050	0.0035	0.0035	900	7.01	20.161	0.71	0.35	4.03
1/600,1/2	0.5	0.0017	0.5	0.0033	0.0024	0.0024	900	4.68	20.161	0.71	0.35	4.03
1/800,1/2	0.5	0.0013	0.5	0.0025	0.0018	0.0018	900	3.51	20.161	0.71	0.35	4.03
1/1000, 1/2	0.5	0.0010	0.5	0.0020	0.0014	0.0014	900	2.81	20.161	0.71	0.35	4.03
1/1200, 1/2	0.5	0.0008	0.5	0.0017	0.0012	0.0012	900	2.34	20.161	0.71	0.35	4.03
1/1600,1/2	0.5	0.0006	0.5	0.0013	0.0009	0.0009	900	1.75	20.161	0.71	0.35	4.03

†Condenser Diameter=D, Volume=V, Height=H, Condenser Area=A, Power=P, Flow Area=FLA, Power per Tube =P_T, Heat transfer Area= HTA, Velocity =v, Reynolds number=Re, Subscript R = prototype to model ratio

4.3 Non-Condensable Effect

For a scaled facility with a power scaling of 1/100, the condenser surface area is scaled by 1/200. Thus for 1/4 height scaled facility, the number of condenser tubes is scaled by 1/50. Since the vapor volume flow rate is scaled by the power scaling, the vapor volume flow rate in scaled facility is scaled by 1/200. Thus with a heat transfer area scaling of 1/200 and boundary mass flow rate scaling of 1/200, we have

$$\left(\frac{N_m}{N_p}\right)_{tube}\left(\frac{N_m}{N_p}\right)_{units}\left(\frac{A_m}{A_p}\right)_i = \frac{1}{200} \tag{4.13}$$

and

$$\left(\frac{\dot{m}_m}{\dot{m}_p}\right) = \frac{1}{200}\ . \tag{4.14}$$

If the temperature differences are preserved in the model, we have from Eq. (4.10) through (4.14),

$$\frac{\left(\dot{Q}_{pccs}/(\dot{m}\, i_{fg})\right)_m}{\left(\dot{Q}_{pccs}/(\dot{m}\, i_{fg})\right)_p} = (U)_R\ . \tag{4.15}$$

As the steam-nitrogen mixture flows into the condenser, the mixture Reynolds number decreases along a tube due to the condensation of the steam. The scaling ratio of the Reynolds number, Re_{mR}, is 1/4. The condensation heat transfer correlation of Siddique et al. [4.1] gives the ratio of h_c to be $h_{cR} = (Re_{mR})^{0.223}$. Thus, for $Re_{mR} = 1/4$, one obtains $h_{cR} = 0.734$. The pool side heat transfer coefficient can be calculated from the standard pool boiling heat transfer correlation. By using the prototypic material for the tubes in the scaled facility, the overall heat transfer coefficient ratio $(U)_R$ is calculated from Eq. (4.2) as 0.833. This indicates that the overall scaled heat transfer in the scaled facility is lower than the prototype by 17%. This is within the uncertainty of the Siddique et al. correlation [4.1] of about 20% relative to its database.

Vierow and Schrock [4.4] developed a correction factor for the condensation heat transfer coefficient of Nusselt based on their experimental data obtained for a vertical tube of

2.2 cm I.D. and 2.1 m in length. It takes into account the effects of noncondensable gas and the mixture Reynolds number as

$$f = \left(1 + 2.88 \text{ x } 10^{-6} \text{ Re}_m^{1.18}\right)\left(1 - 0.938c^{0.13}\right). \quad (4.16)$$

The application of this correlation shows that the overall scaled heat transfer in the scaled facility is about 30% lower than in the prototype system when the original geometrical scales given by the global scaling criteria are maintained.

4.4 References

4.1 Siddique, M., Golay, M.W., Kazimi, M.S., "Local Heat Transfer Coefficients for Forced Convection Condensation of Steam in a Vertical Tube in the Presence of a Noncondensable Gas," Nuclear Technology, Volume 102, p386-402 (1993).

4.2 GE Nuclear Energy, "SBWR Standard Safety Analysis Report," Report No. 25A5113 Rev. A, August, (1992).

4.3 Ishii, M., Revankar S. T., Dowlati, R.,. Bertodano, M. L., Babelli, I., Wang, W., Pokharna, H., Ransom, V. H., Viskanta, R., Wilmarth, T., Han, J. T.," Scientific Design of Purdue University Multi-Dimensional Integral Test Assembly (PUMA) for GE SBWR," Purdue University Report PU-NE-94/1, U.S. Nuclear Regulatory Commission Report NUREG/CR-6309, (1996).

4.4 Vierow, K.M., Schrock, V.E., "Condensation in a Natural Circulation Loop with Noncondensable Gases Part 1 - Heat Transfer," Proceeding of the International Conference on Multiphase Flows '91-Tsukuba, p183-186 (1991).

5. EXPRIMENTAL PROGRAM

The experimental program consists of design of the experimental loop, setting up experimental procedures, performing condensation tests with and without non-condensable gas and data analysis.

5.1 Experimental Loop

The schematic of the experimental set-up is shown in Figure 5.1. The test loop is comprised of steam generating tank, steam meter, air supply, instrumented condenser test section with annular cooling jacket, condensate/separator tank and associated piping. The schematic of the condenser tube is shown in Figure 5.2. The specific design of the PCCS condenser tube was based on the scaling analysis presented in chapter 4. Two tubes sizes are considered; 2.54 mm ID and 5.04 mm ID. A height scaling of ½ was taken in the present design.

The steam supply vessel is made of schedule 10, 16-inch diameter stainless steel pipe. Its total length is 2.26 m. An immersion type sheathed electrical heater of 10kW capacity is mounted at the lower flange of this vessel. The vessel is instrumented with thermocouples, P and DP cells to measure and monitor temperature, pressure and water level. The boiler vessel design is shown in Figure 5.3.The power to the heater is measured with a.c. Voltmeter and ammeter. The steam supply line to the condenser is made of 2.54 cm (1 inch) stainless steel pipe. The A compressed air is supplied to the steam line through a flow control valve. This feed line supplies air-steam mixture to the test section. The test section is designed using a double annulus with stainless steel condensers tube and an outer jacket also made of stainless steel. The design drawings of the 5.04 cm (2-inch) condenser tube are shown in Figure 5.4. The condenser jacket is shown in Figure 5.5 and assembly of the condenser and the outer jacket is shown in Figure 5.4. The test section is fitted with thermocouples mounted on annulus inner and outer wall to measure local temperature. The condenser tube wall will have flush mounted thermocouples on inside and outside wall surface distributed in radial and at several axial locations. The condensate tank serves as separator and condensate collector. It is made of Schedule 10, 12-inch pipe and is mounted vertical. The design drawing of the condensate tank is shown in Figure 5.6. The water level in the condensate tank can be maintained at desired level by continuous bleeding water from the tank. The condenser operating pressure is set by the pressure level in the condensate tank. An airline is connected to the condensate tank to set the pressure higher than the atmosphere pressure.

Table 5.1 summarizes various parameters measured and the instruments.

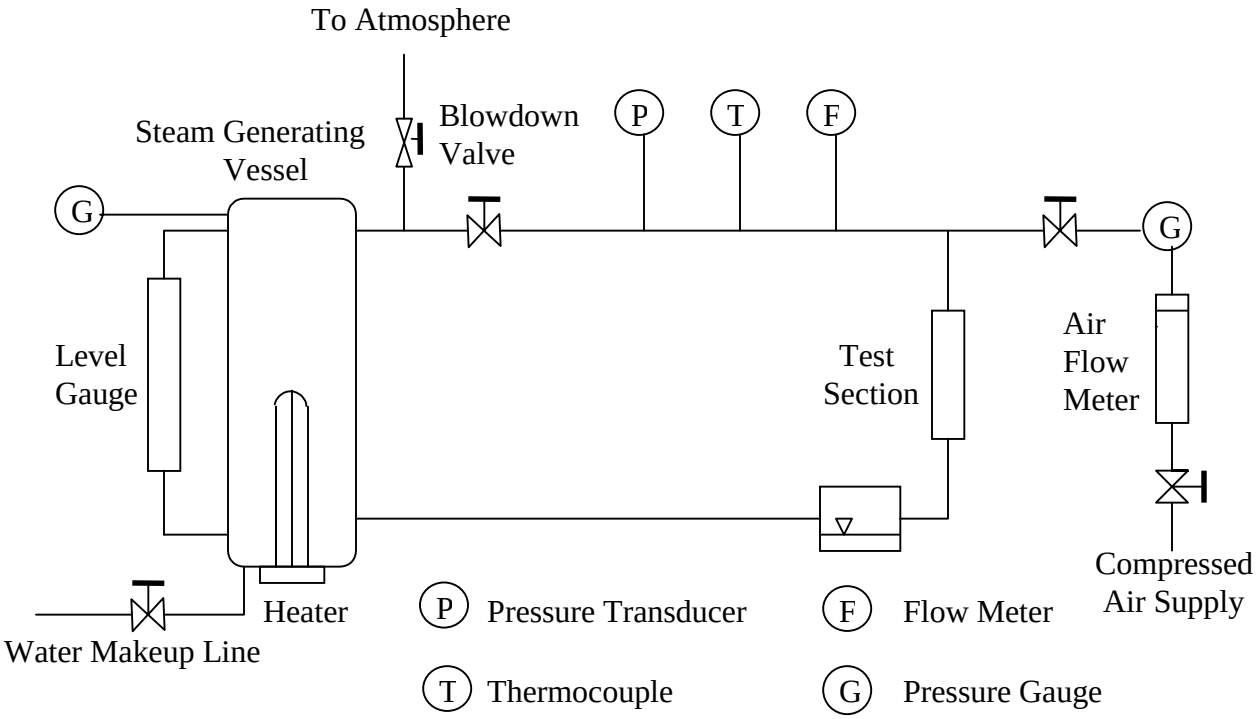

Fig 5.1 Schematic of the Experimental Setup

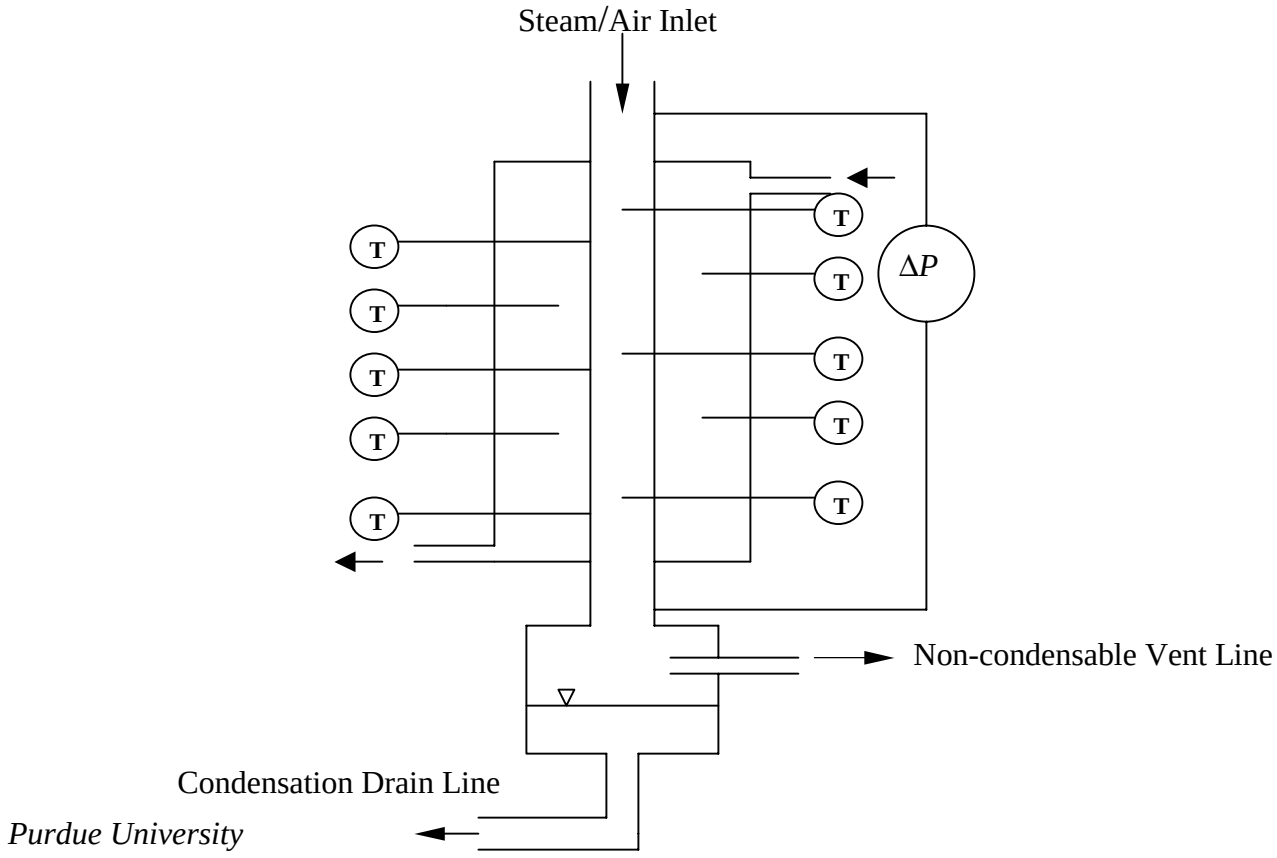

Fig 5.2 Schematic of Condenser

Table 5.1 List of Instruments

Data	*Instrument*
Steam Flow Rate	Vortex Flow Meter.
Air Flow Rate	Rotameter
Power	Voltmeter and Ammeter
Condensation rate	Catch Tank Method
Pressure Water Level	Pressure Transducer DP cell
Temperature	Thermocouples
Heat Loss from Wall	Heat Flux Sensors

5.2 Experimental Method:

Experiments are performed for the following flow conditions: (1) Forced convection flow, (2) Continuous condensation mode where no through flow of vapor occurs and (3) Cyclic Condensation Mode. In the third mode of operation the non-condensable is left to accumulate in the condenser and is vented automatically when the pressure in the condenser tube is larger than the head at the submerged vent line. The cycle of venting is determined by the non-condensable fraction. Experimental parameters include, inlet steam flow rate, inlet non-condensable gas concentration (0-20%), operating pressure (100-1000 MPa), and secondary coolant temperature (50^{o} C - 100^{o}C).

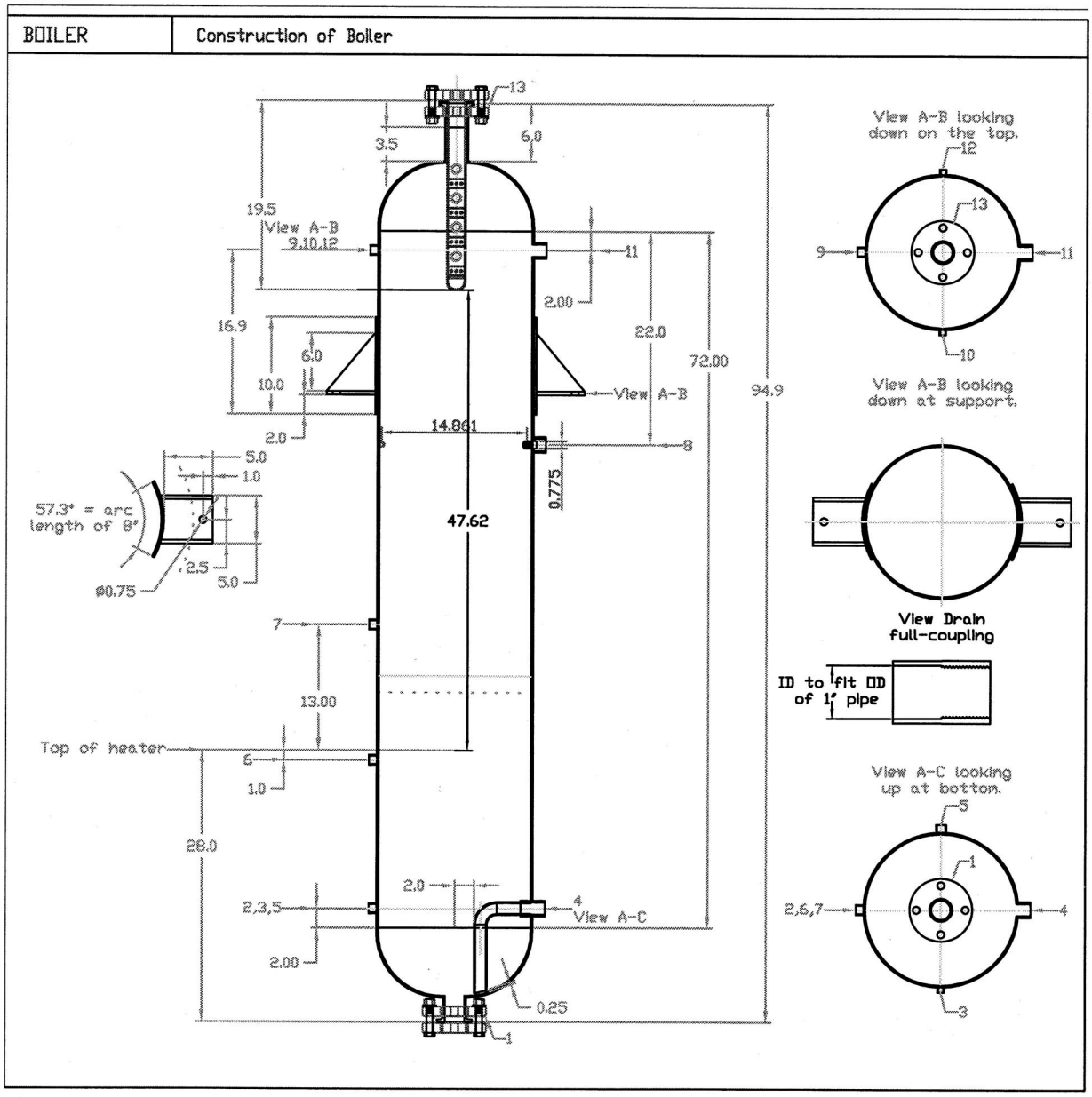

Figure 5.3 Boiler Vessel Design

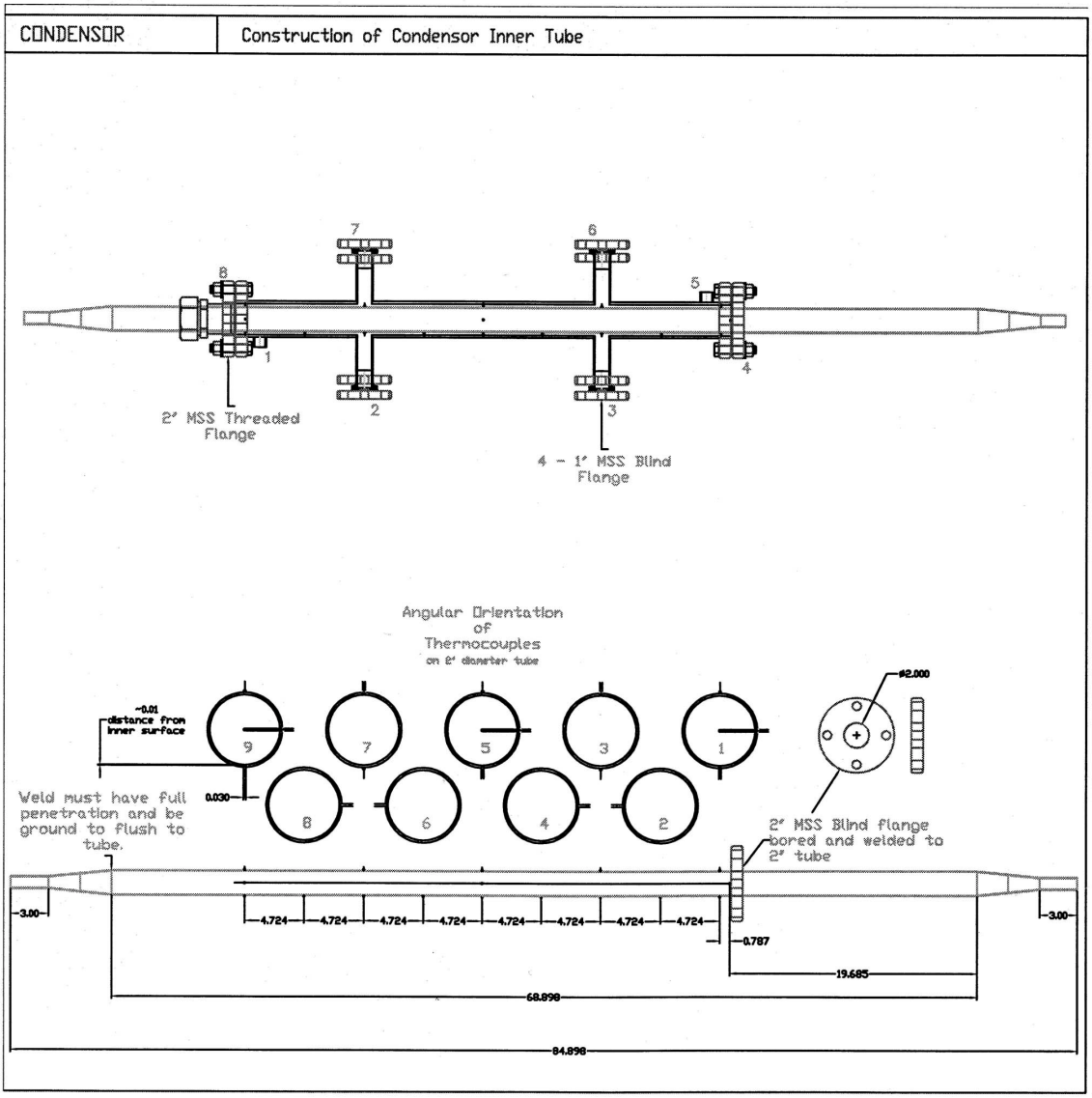

Figure 5.4 5.04 cm Condenser Tube Design and Assembly

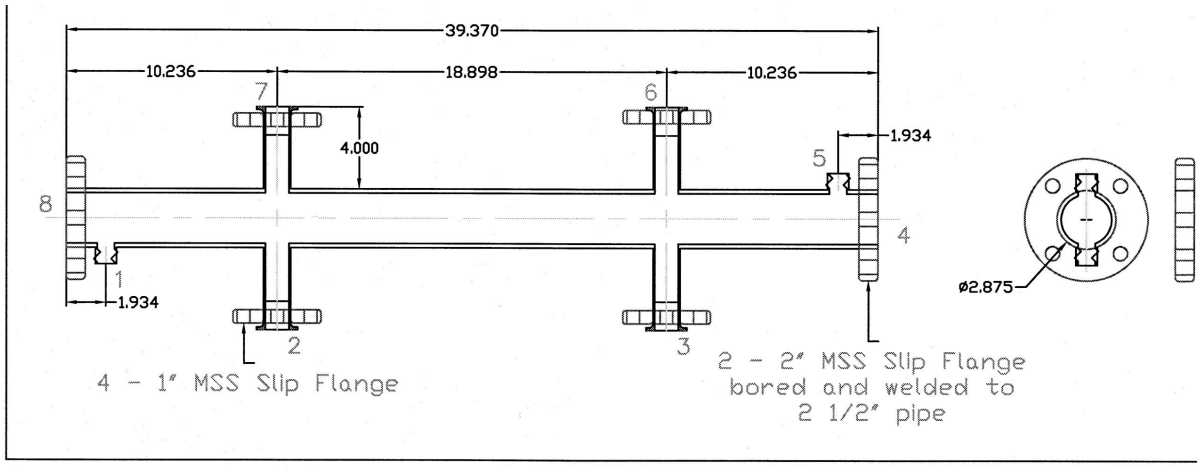

Figure 5.5 Condenser Outer Jacket Design

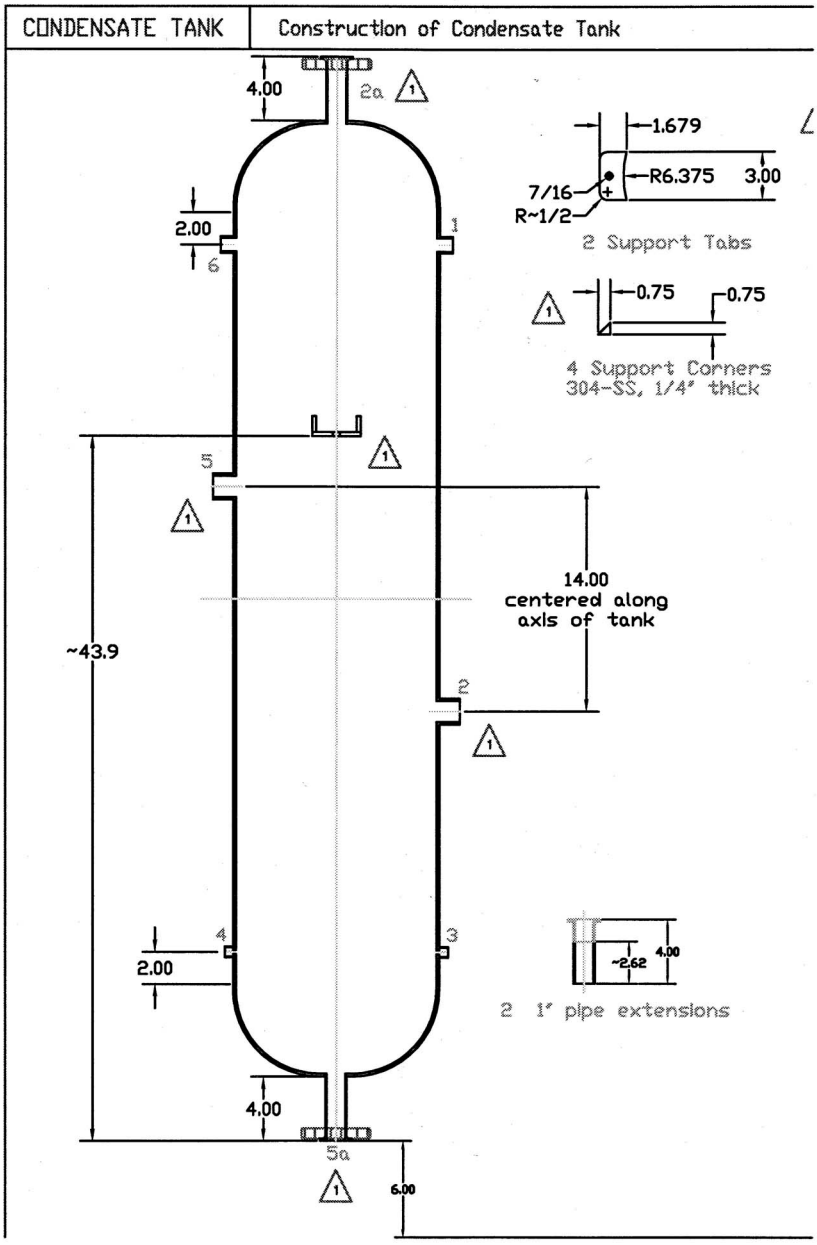

Figure 5.6 Condensate Tank Design

6. ANALYTICAL MODELING

In this task an analytical model was developed for the condensation in vertical tube. A convective film-wise condensation of a vapor and non-condensable gas mixture flow downward inside a vertical tube was studied. A unified procedure was developed to predict the condensation heat transfer coefficient of turbulent vapor flow associated with laminar condensate. The predictions were compared with the experimental data in the literature. Parameters such as the, temperature, and gas mass fractions were presented in axial and radial profiles.

6.1 Introduction

Many industrial systems use vertical tube condensers and industrial practice has indicated that, often, much higher coefficients of heat transfer are obtained when vapors are condensed inside tubes rather than outside [6.1]. However, in practical operations of the condensers, small amounts of non-condensable gas may exist in working vapors due to characteristics of the system or dissolution of working vapors. It is well known that the presence of non-condensable gases in a vapor can greatly reduce the performance of condensers [6.2-6.8]. This is because of the fact that the presence of non-condensable gas lowers the partial pressure of the vapor, thus reducing the saturation temperature at which condensation occurs.

Thus, predicting the effects of non-condensable gas in annular film-wise condensation of vapors in a vertical tube is an important technical and theoretical interest. The condensation of vapors from a vapor-gas mixture in a tube has been studied by various authors [6.3,6.10-6.20]. The analysis of the heat and mass transfer during condensation of a vapor in the presence of a non-condensable gas has generally involved either the boundary layer analysis or the heat and mass transfer analogy methods. In both of these methods the condensation is viewed as occurring in two interacting boundary layers, the vapor-air mixture and the condensate boundary layers. The boundary layer solutions currently available deal primarily with the flat plate configuration and stagnant atmospheric conditions [6.21,6.22].

The analysis of the heat and mass transfer analogy models follow the general methodology of Colburn and Hougen [6.3,6.14-6.16]. Ghiaasiaan et al. [6.17] presented a two-fluid model for condensation in the presence of non-condensable gas in a channel. The condensate-gas interphase heat, mass and momentum transfer, are treated using the stagnant film model. This methodology requires interphase surface area concentration and liquid and gas side transfer coefficients.

Condensation in the presence of non-condensable gas has recently been experimentally studied in tube flow configuration by Vierow [6.23], Ogg [6.24], Siddique [6.25] and Kuhn et al [6.26], because of its application in various industrial systems. From the survey it is evident that no analytical treatment exists that is free from a semi-empirical approach and which is consistent with the process of condensation (including laminar and turbulent film flow) inside a vertical tube in the presence of non-condensable gas. In view of this, the present work deals with convective film-wise condensation of a vapor and gas mixture flow downward inside a vertical tube. A unified procedure is developed to predict the condensation heat transfer coefficient of turbulent vapor flow associated with laminar condensate. The predictions are compared with the experimental data in the literature.

6.2 Condensation Model

In this section the physical model for the condensation process is described. The governing equations for the mass, momentum, energy, and species concentration balance are presented along with the interface and boundary conditions. The basic assumptions used in the present model are given. The model is similar to Chen and Ke [6.27] and Wang and Tu [6.14] models for pure vapor condensation. The non-condensable effects on the condensation are taken into account through boundary layer analysis of species concentration and energy balance similar to Minkowycz and Sparrow [6.22].

Assumptions:

1. The flow is two-dimensional and steady state.
2. The cross sectional geometry is circular and axially uniform.
3. The condensate film is impermeable to non-condensable gas.
4. The wall temperature is known.
5. The non-condensable gas is assumed to be locally well mixed and at thermodynamic equilibrium with the vapor.
6. The vapor - non-condensable mixture is assumed to be saturated with vapor.
7. The mass exchanged because of phase change at the liquid-gas interface has the properties corresponding to the interphase temperature
8. The properties of the vapor-gas mixture are assumed to be constant except at the boundary layer near the film interface.

Physical Model

Figure 6.1 shows the schematic of the physical model considered for the condensation process with defined coordinate systems. A saturated vapor-gas mixture, with constant properties corresponding to inlet pressure and temperature conditions, enters the tube and is turbulent. The condenser tube surface is below the vapor saturation temperature. The condensate forms along the tube surface and thus an annular flow regime is realized inside the condenser tube. Along the condensate film interface, a temperature, momentum and concentration boundary layers develop and respective gradients are formed. These gradients are shown later to impede the condensation.

Conservation of Mass

The mass conservation equation for the vapor-gas mixture is

$$\frac{\partial \rho r v}{\partial r} + \frac{\partial \rho u}{\partial x} = 0 . \tag{6.1}$$

Since we have assumed constant properties for the vapor-gas mixture, the density can be taken out of the equation. This equation is used with the momentum equation to check mass conservation. Therefore an equation is needed to relate the average axial velocity and the radial velocity. This is obtained by integrating eq. (6.1) from the centerline to essentially the wall. The film thickness is assumed negligible compared to the radius.

The boundary conditions for the radial velocity term are v = 0 at the centerline and v_i at the wall. The gradient of the average axial velocity is obtained as:

$$\frac{d\bar{u}}{dx} = -\frac{2v_i}{R} \tag{6.2}$$

For a very small condensation velocity, v_i, it is assumed that velocity profiles are locally self-similar as given by Kinney and Sparrow [6.28]:

$$u/u_{avg} = f\,(r/R) \tag{6.3}$$

From eqs. (6.2) and (6.3) the following is obtained:

$$\frac{\partial u}{\partial x} = -\frac{2v_i u}{R\bar{u}} \quad . \tag{6.4}$$

Substituting this into eq. (6.1) a radial velocity profile is derived as:

$$(R - y)\frac{\partial v}{\partial y} - v = \frac{2(R - y)v_i u}{R\bar{u}} \quad . \tag{6.5}$$

Conservation of Momentum

The momentum conservation equation is given as:

$$\rho\ [r\frac{\partial u^2}{\partial x}+\frac{\partial ruv}{\partial r}]=-r\frac{\partial p}{\partial x}-\frac{\partial r\tau}{\partial r}+g(\rho_l-\rho)\ . \tag{6.6}$$

This equation is used to obtain the radial velocity profile. The effect of gravity is neglected, as the flow is forced convection. For turbulent flow, the shear stress is normally written as a function of the velocity gradient and is written in the following:

$$\tau\ =-\rho\ (\nu\ +\varepsilon_m)\frac{\partial u}{\partial r}\ . \tag{6.7}$$

The corresponding boundary conditions are:

$$v = v_i \text{ and } \tau = \tau_i \qquad \text{at } r = R-\delta \text{ or } y =\delta$$

$$\partial u/\partial r = 0 \qquad \text{at } r =0 \qquad \text{or } y = R\ . \tag{6.8}$$

Here it is assumed that the tube radius is larger than the film thickness ($R>>\delta$), and that the average mixture velocity, u_{avg}, is also larger than the interface velocity ($u_{avg}>>v_i$). These assumptions are reasonable since the liquid density is much larger than the mixture density.

The turbulence model of vapor flows in this work incorporates the main features of Kinney and Sparrow's [6.28] work but with a key difference. The difference is the inclusion of the effect of the interface damping on eddy transport as deduced from gas absorption data. The pressure gradient term in the momentum equation is eliminated using similar approach proposed by Kinney and Sparrow [6.28].

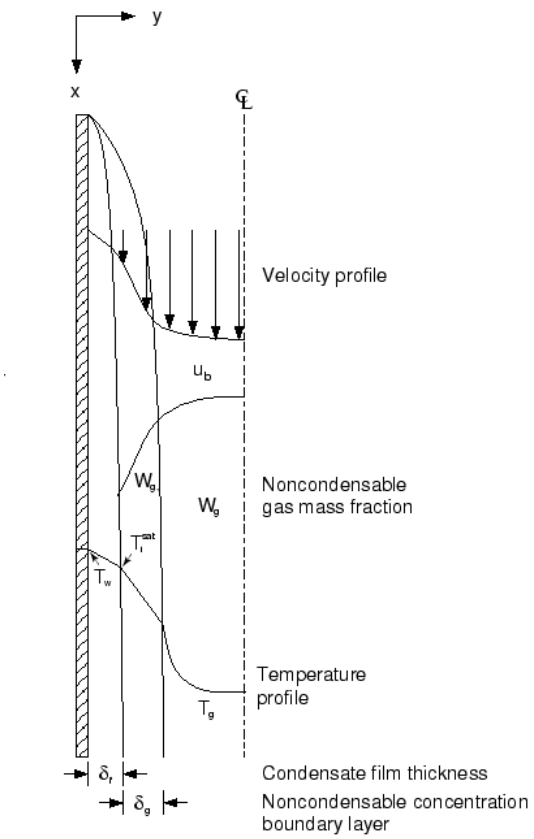

Figure 6.1 Flow Geometry.

From eqs. (3)-(7), the integro-differential equation for the turbulent vapor flow is obtained as:

$$\left(1+\frac{\varepsilon_m}{\nu}\right)\frac{du^+}{dy^+} =$$
$$-\left[\frac{2Nv_i}{R^+(R^+-y^+)\bar{u}}\left[\int_0^{R^+} u^+(R^+-y^+)dy^+ - \int_0^{y^+} u_g^+(R^+-y^+)dy^+\right]\right]*\frac{u^+}{r^+}+$$
$$+\left[\frac{r^+}{R^+}\left(\frac{\tau_i}{\tau_w}\right)DN+4N\left(\frac{v_i}{\bar{u}}\right)\left(\frac{1}{R^+r^+}\right)\right.$$
$$\left.+\left[\left[\left(1-\frac{r^+}{R^+}\right)^2\int_0^{R^+} u_g^{+2}\left(R^+-y^+\right)dy^+ - \int_0^{y^+} u^{+2}\left(R^+-y^+\right)dy^+\right]\right]\right. \qquad (6.9)$$

where $u^+ = u/u^*$, $y^+ = yu^*/\nu_l$, $R^+ = Ru^*/\nu_l$, $u^* = (\tau_w/\rho_l)^{1/2}$, $D=\rho_l/\rho_g$, $N = \nu_l/\nu_g$.

Using the method employed by Kinney and Sparrow[28], the pressure gradient term is now derived and contains both the interfacial shear and momentum flux terms :

$$Re_g = \frac{4N}{R^+}\int_0^{R^+} u_g^+\left(R^+ - y^+\right)dy^+ \qquad c_f = 2DN^2\left(\frac{2R^+}{Re_g}\right)^2$$
$$\frac{dP}{d\frac{x}{2R}} = -\frac{1}{2}\rho\bar{u}^{\,2}\left[4c_f - 16N^2\left(\frac{v_i}{\bar{u}}\right)\frac{8}{Re_g^2}\int_0^{R^+} u^{+2}\left(R^+ - y^+\right)dy^+\right] \tag{6.10}$$

Conservation of Energy

The energy conservation equation is required to find the temperature gradient at the interface. This gradient is the driving force for condensation. The energy conservation equation was given by Minkowycz and Sparrow [6.22] for flat plate geometry. Here, for cylindrical geometry, the energy conservation equation is given as,

$$\rho c_p\left[\frac{v}{r}\frac{\partial rT}{\partial r} + u\frac{\partial T}{\partial x}\right] + \frac{(c_{pg} - c_{pv})j_g}{r}\frac{\partial rT}{\partial y} = -\frac{1}{r}\frac{\partial q^*}{\partial x}$$
$$\text{where} \qquad q^* = -\frac{k}{r}\frac{\partial rT}{\partial y} + \alpha\frac{RTM^2}{M_g M_v}j_g \tag{6.11}$$
$$j_g = -\rho D\left[\frac{1}{r}\frac{\partial rW}{\partial y} + \frac{\alpha W(1-W)}{Tr}\frac{\partial rT}{\partial y}\right] \quad .$$

The $(c_{pg}\text{-}c_{pv})j_g dT/dy$ term represents the net enthalpy flux owing to the diffusion currents. The q* equation includes both the conductive term and a diffusive term. The j_g term has a mass diffusion term and a thermal diffusion term. The following are the boundary conditions,

$$T = Ti \qquad \text{at } r = R$$
$$dT/dy = 0 \qquad \text{at } r = 0 \ . \tag{6.12}$$

Conservation of Species

Finally the last conservation equation needed for a complete solution is the species conservation. In a binary mixture, mass must be conserved for each of the components. This requirement may be satisfied by writing a diffusion equation for each of the species, or alternately a continuity equation for the mixture and a diffusion equation for one of the species. The latter is used in this present model.

In a two-component gas mixture it is convenient to represent the local concentrations in terms of the mass fractions and they are defined as

$$W_g = \rho_g/\rho \qquad W_v = \rho_v/\rho \ , \tag{6.13}$$

where, $\rho = \rho_g + \rho_v$ and then $W_g + W_v = 1$.

Here for simplicity the symbol W will be used as the gas mass fraction. Since there are concentration and temperature gradients due to the noncondensable gas near the interface a mass diffusive flux, j_g, term is needed. A similar expression can be written for the vapor and is the negative of the gas diffusive flux. The general form of the species conservation equation is:

$$\rho\left(u\frac{\partial W}{\partial x} + \frac{v}{r}\frac{\partial rW}{\partial r}\right) = -\frac{1}{r}\frac{\partial j_g r}{\partial r}$$
$$\text{where } j_g = -\rho D\left[\frac{1}{r}\frac{\partial rW}{\partial y} + \frac{\alpha W(1-W)}{Tr}\frac{\partial rT}{\partial y}\right] \tag{6.14}$$

The boundary conditions for this equation are:

$$W = Wi \qquad \text{at } r = R\text{-}\delta \text{ or } y = \delta$$
$$\partial W/\partial y = 0 \qquad \text{at } r = 0 \text{ or } y = R \tag{6.15}$$

Here, α is not the thermal diffusivity but a thermal diffusion coefficient and is given in Mason and Monchick [29].

Interfacial Terms

Four important interfacial parameters govern the rate of condensation. These are the interfacial radial velocity, temperature, gas mass fraction, and film thickness. The expressions for these parameters are given in the following.

Peterson et al.[6.30] have developed a diffusion layer theory to describe condensation in the presence of non-condensable gases. They presented an expression for the average condensation velocity as

$$v_i = \frac{Dh_{fg}M_v x_{v,avg}}{RT^2_{avg} x_{g,avg}\delta_g}(T^s_i - T^s_b) \ . \tag{6.16}$$

This equation is based upon Fick's Law and the ideal gas law and here it is used to determine interface velocity, v_i.

One of the important parameters is the film thickness. The energy balance at the mixture-liquid interface is given as:

$$mh_{fg} = h_l(T_i - T_w) \qquad (6.17)$$

where the heat transfer coefficient is derived by a simple energy balance at the wall

$$-k_l \frac{dT}{dy}_w = h_l(T_b - T_w) \quad .$$

Assuming the temperature in the liquid film is linear, the heat transfer coefficient is expressed as:

$$h_l = \frac{(T_i - T_w)k_l}{(T_b - T_w)\delta} \qquad (6.18)$$

Substituting h_l from this equation in eq. (6.12) we get an equation for δ using $m = v_i\rho$,

$$\delta = k_l(T_i - T_b)/v_i\rho h_{fg} \quad . \qquad (6.19)$$

Using these equations a Nusselt number can be derived as,

$$Nu_l = 2h_lR/k_l \qquad (6.20)$$

Two more required parameters at the interface are gas mass fraction and temperature. These are related by the following equation derived using the ideal gas law.

$$\frac{P_v}{P} = \frac{1-W}{1-W(1-M_g/M_v)} . \qquad (6.21)$$

From this equation, one parameter is determined by assuming the other. Each parameter in the interfacial equations all depends upon one another. The least dependent variable is either the gas mass fraction or the interfacial temperature. Therefore if one parameter is assumed, the other three parameters can be determined.

Turbulent Transport Model

As outlined in Yih and Liu [6.31], the eddy diffusivity of momentum is divided into two parts for the mixture region. These are the outer region, from $y^+>26$, and the interface region, $y^+<26$. The outer region is given as,

$$\frac{\varepsilon_m}{\nu} = \frac{y^+}{2.5} . \qquad (6.22)$$

The interface region is given as,

$$\frac{\varepsilon_m}{\nu} = 6.47X10^{-4}\frac{g\rho}{\sigma}\left(\frac{\nu_l}{u^*}\right)^2(\delta^+ - y^+)^2 Re^{1.678} . \qquad (6.23)$$

6.3 Solution Methodology

The coupled integro-differential equations derived above were solved using finite difference scheme as given in Patankar [6.32].

Inlet Conditions

The specified inlet conditions are the mixture Reynold's number, entrance total pressure, and gas mass fraction. The geometric parameters to be specified are the tube radius and length. The key boundary condition is the tube wall temperature. The node lengths in the radial and axial directions are specified based on numerical accuracy required. The vapor partial pressure is calculated from the total pressure and from the gas mass fraction. The mixture temperature is then obtained as the saturation temperature corresponding to the vapor partial pressure. The fluid transport properties such as viscosity, thermal conductivity, thermal diffusion factor, binary diffusion coefficient, and surface tension are calculated using the mixture temperature at the gas core.

With the fluid properties known, the inlet axial velocity is calculated from the specified Reynold's number. A flat mixture velocity profile is assumed at the entrance. Corresponding gas mass fraction and temperature profiles are also assumed to be flat at the entrance. Temperature profile is thus the temperature determined from the vapor partial pressure. Thus all required parameters are determined for the inlet conditions. This nodal position is termed as the first axial node.

Parameter Initialization for the Next Set of Nodes

Next parameter initialization is needed to start the calculation procedure at the downstream node (e.g. second node) as they are unknown beforehand. For the second set of nodes, a pressure difference is calculated using the entrance velocity and Reynolds number from the following equation

$$\frac{dP}{dx} = -\frac{1}{2}\frac{\rho\bar{u}^2}{2R} f_0 ; \quad \text{where} \qquad f_0 = \frac{.079}{Re^{1/4}} \tag{6.24}$$

A new total pressure is calculated for the second set of nodes. Then using the inlet gas mass fraction the vapor partial pressure is determined for the second node and the required properties are calculated for this second node. In the initialization, the effect of the noncondensible gas is neglected. Therefore the interfacial velocity is assumed and the condensate film thickness is calculated using eq. (6.19). The inlet velocity is used as the velocity profile for the second node.

The wall shear stress and the interfacial shear stress are calculated following Dobran and Thorsen [33]:

$$f_0 = \frac{.079}{Re_g^{.25}}; \quad f = f_0\left(1+300\left(\frac{\delta}{2R}\right)\right)$$
$$\tau_i = \frac{1}{2}\rho\bar{u}^2 f \tag{6.25}$$
$$\tau_w = \left((\rho_l - \rho)g - \frac{dp}{dx}\right)\delta + \tau_i$$

Once these values are known, the value of u* is calculated and all variable are converted into their non-dimensional form. Then a new non-dimensional velocity profile is calculated for the second node. This process is repeated for each subsequent node. At each node, the continuity and energy balance equations are satisfied.

6.4 Results And Discussion

In order to validate the present model, the model predictions were compared first with experimental data on forced convection pure steam condensation. Then the present predictions were compared with steam-air condensation in a vertical tube.

Pure Steam Data Comparison

Three sets of pure steam condensation data from experiments done by Goodykoontz and Dorsch [34] are available. These involve different conditions in temperature and Reynold's numbers. The inlet conditions and results of the experiment and results obtained by the present model are summarized in Table 6.1. The average Nusselt number from the present model was calculated by taking the area average of the local Nusselt number as

$$Nu_{l,avg} = \frac{\int_0^x Nu(x)xdx}{\int_0^x xdx}.$$

The predicted Nusselt number compares very well with two of the cases (case 1 and case 3) and does better than the results obtained by Dobran and Thorsen [6.33]. Case 2 was off by a factor of almost 2. This is attributed to the fact that the present model did not calculate for the

entire tube length, because of the low steam velocity. The solution convergence was not attained once the steam velocity became too low.

Table 6.1 Inlet Conditions and Results for Goodykoontz and Dorsch [34] Data

#	T_{sat} (K)	Re E4	T_{wall} (K)	P (Pa) xE5	Nu exp	Nu pred.	Error (%)
1	401	7.99	374	2.53	266	235.4	11.5
2	403	3.58	379.5	2.69	112	189.2	68.9
3	400	4.46	370.5	2.45	154	168.2	9.2

The local axial Nusselt number predictions are shown in Fig. 6.2. The Nusselt number decrease farther away from the inlet. From Table 6.1 it is seen that case 2 and case 3 are very similar, but the Nusselt number varies greatly in experimental results. The model predictions, however, show comparable heat transfer coefficients for case 2 and 3. Thus it is concluded that the model predictions are consistent. The reasonable agreement of the model prediction in this experimental data is taken as the validation of the present model for pure vapor condensation.

Comparison with UCB and MIT Steam-Air Condensation Data

Table 6.2 shows the condenser geometry and inlet conditions for the UCB and MIT experiments [23]. In Fig. 6.3, the model predictions are compared with the experimental data for non-condensable concentration of 10%. It is seen that the model does fairly well predicting the experimental data. The experimental data itself contains errors as well. It should be noted that there is a large scatter in MIT data. In Fig. 6.4 the model predictions are compared with the UCB and MIT data for non-condensable gas concentration of 20%. In spite of the data scatter the predictions shows reasonable agreement with the experimental data.

In order to gain insight into the effects of the local parameters on the condensation, the model predicted radial profiles for temperatures and non-condensable gas concentration are shown for the UCB test conditions with $W_{in} = 0.1$ in Figs. 6.5 and 6.6 respectively.

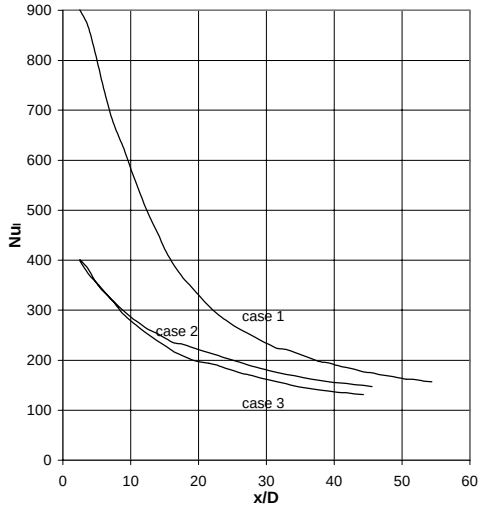

Figure 6.2. Local Nusselt Number Predictions for the Pure steam Condensation Experiments of Goodykoontz and Dorsch [34].

Table 6.2 Inlet Conditions for MIT [25] and UCB [23] Experiments

Case #	D (m)	L (m)	P (Pa)	W_{in} (%)	Re_g	T_{wall} (K)
UCB	.022	2.54	2E5	10, 20	2E4	373
MIT	.046	2.54	2E5	10, 20	2E4	373

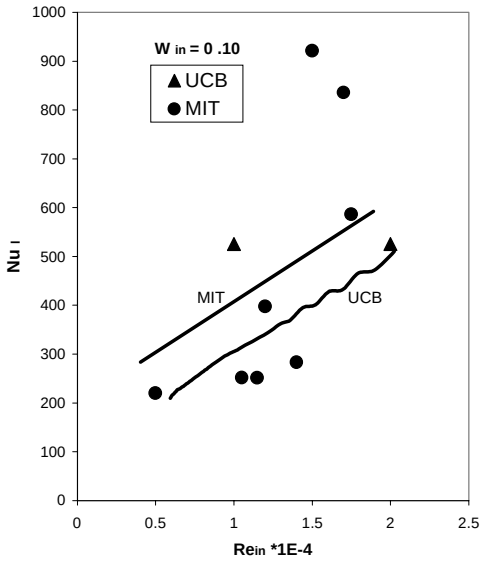

Figure 6.3. Comparison of Model Prediction with MIT and UCB Data for W_{in} =10%.

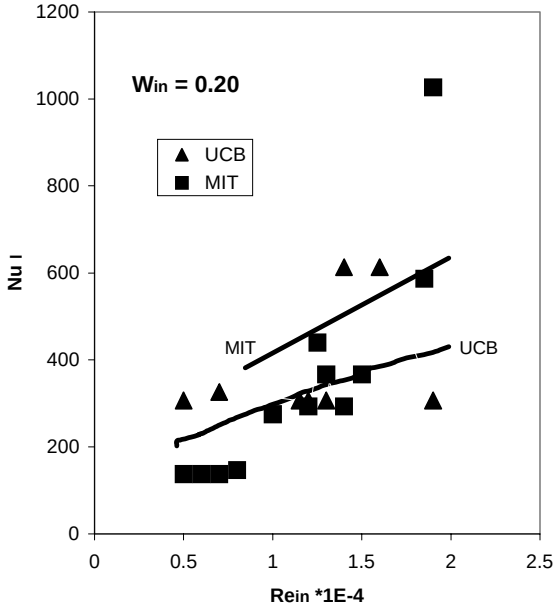

Figure 6.4. Comparison of model prediction with MIT and UCB data for W_{in} =20%.

These profiles are typical for both MIT and UCB data and hence only predictions for UCB are shown here. There is substantial drop in the temperature at the interface due to the buildup of the gas. This is an indication of how much the heat transfer is impeded. It is also seen that the thermal boundary layer thickness increases with x/D. This is due to increase in the gas layer thickness along the length of the tube. The radial gas mass fraction profile properly compliments the temperature profile; .the gas buildup near the interface is clear from this figure. Here again the boundary layer for species concentration increases with x/D. The bulk concentration does not change.

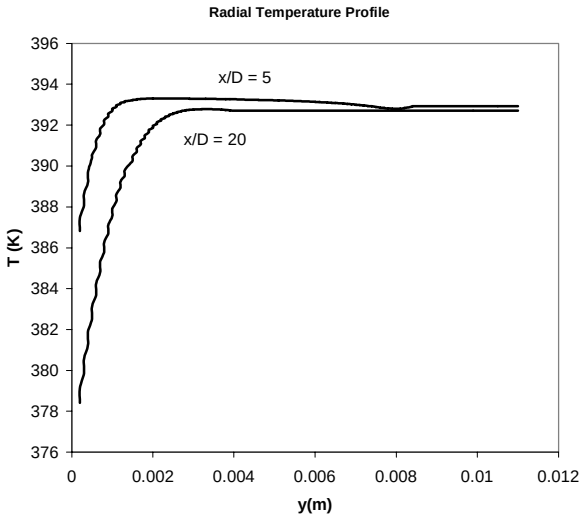

Figure 6.5. Model Predicted Radial Temperature Profile for UCB Case with 10% Gas Mass Fraction at x/D=5 and 20.

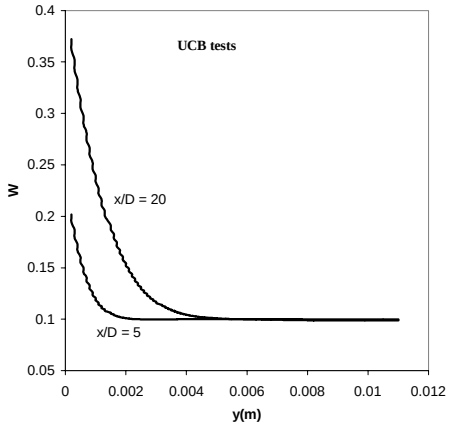

Figure 6.6 Model Predicted Radial Gas Mass Fraction Profile for UCB Case with 10% Gas Mass Fraction at x/D=5 and 20.

The condensation of steam in the presence of non-condensable gas reduces as a result of the build up of the gas near the interface. As seen from the predicted radial profile the gas concentration increases near the condensate film interface along the downstream end of the flow. In Fig. 6.7 the interface gas mass fraction is shown along the tube length for inlet gas concentrations of 10% and 20%. A linear increase in interface gas concentration is seen from these predictions.

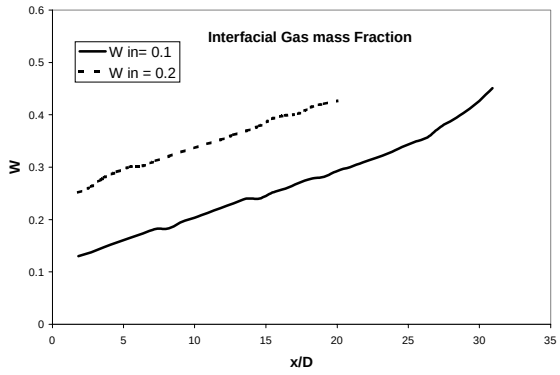

Figure 6.7. Model Predicted Interface Gas Mass Fraction as a Function of Tube Length.

6.5 Conclusions

A detailed physical model for vertical tube condensers with forced convection of vapor-non-condensable gas mixture was developed. The model assumed an annular flow regime in the tube with turbulent core mixture flow. Reasonable assumptions were made in describing the physical model. The conservation equations for mass, momentum, energy, and species concentration were developed. The equations were then simplified into integro-differential equations using well-tested mathematical techniques. A heat transfer balance equation was developed at the film-gas interface. For heat transfer at the interface in the presence of the non-condensable gas, a diffusive boundary layer model was used. This model enables the relation of the condensate velocity with the temperature at the interface.

Test cases for pure steam condensation were studied and the predicted heat transfer results were compared with the experimental data. The prediction and the experimental data of Goodykoontz and Dorsch [6.34] agree very well. The model was thus validated against experimental data.

Test cases of condensation in the presence of non-condensable gas, air, were studied at high gas mass fractions (10% and 20%). The results of the predictions were compared to the experimental data of UCB [6.23] and MIT [6.25]. The agreement was fairly good.

6.6 References

6.1.Wurster, A., 1942, In " Discussion", Trans. American Institute of Chemical Engineering, 38, pp. 464-468 .

6.2.Morgan C.D., 1983, "Analysis of Condensation Heat Transfer with Non-condensable Gases Present in a Vertical Tube at High Pressure," presented at 21st National Heat Transfer Conference, Seattle, Washington, ASME HTD, Vol. 27, pp. 24-28.

6.3.Colburn A.P. and Hougen O.A, 1934, "Design of Cooler Condensers for Mixture of Vapors with Noncondensing Gases, "Industrial and Engineering Chem. 26, pp. 260-267,

6.4.Sparrow, E.. M. Minkowycz, W. J. and Saddy M., 1967, "Forced convection condensation in the presence of a noncondensible gas and interfacial Resistance," International Journal of Heat and Mass Transfer, 10, pp. 1829 - 1845.

6.5.Morgan, C.D. and Rush G.C., 1983, "Experimental Measurements of Condensation Heat Transfer with Noncondensible Gases Present," presented at 21st National Heat Transfer Conference, Seattle, Washington, ASME HTD Vol. 27, July 24-28.

6.6.Borishanskiy V.M and Volkov O. P., 1977, "Effect of Uncondensible Gases Content on Heat Transfer in Steam Condensation in a Vertical Tube," Heat Transfer - Soviet Research 9, no.2, pp. 35 - 41,

6.7.Hein D., Rippel R. and Weiss P., 1982, "The Distribution of Gas in a U-Tube Heat Exchanger and its Influence on the Condensation Process," Proceedings of the Seventh Int. Heat Transfer Conference, Munchen, Germany Vol. 5, pp. 467-473.

6.8.Collier J.G., 1981, *Convective Boiling and Condensation,* 2nd Edition, McGraw-Hill London.

6.9.GE Nuclear Energy, 1982, SBWR Standard Safety Analysis Report, 25A5113, Rev A.

6.10. Baasel W.D and Smith J.C, 1962, "Mathematical Solution for the Condensation of Vapor from Noncondensing Gases in Laminar Flow inside Vertical Cylinders," AIChEJ, 9 pp. 826-830.

6.11. Cossman R., Odenthal H. P. and Renz U, 1982, "Heat and Mass Transfer During Partial condensation in a Turbulent Pipe Flow," Proceedings of the Seventh Int. Heat Transfer Conference Vol. 5, pp. 53-58.

6.12. Westwater J.W., 1983, *Condensation, In Heat Transfer in Energy Problems*, Edited by T. Mizushina and W.J. Yang, Hemishphere, Washington DC, pp. 81-92.

6.13. Wang C. Y. and Tu C. J., 1987, "Heat Transfer and Pressure Drop for Laminar Two-Phase Flow During Condensation with Non-Condensable Gas in a Tube, "Proceedings of Sino-US International Symposium on Multiphase Flow, August 3-5, Zhejiang University Press, Hangzou.

6.14. Wang C. Y. and Tu C. J., 1988, "Effects of Noncondensible Gas on Laminar Film Condensation in a vertical tube," International Journal of Heat and Mass Transfer, 31 no. 11, pp. 2339 –2345.

6.15. McNaught J. M., 1979, "Mass Transfer Correction Terms In Design Methods for Multi Component/ Partial Condensers," Condensation Heat Transfer -ASME, New York, p 11.

6.16. Siddique M., Golay S. and Kazimi M., 1994, "Theoretical Modeling of Forced Convection Condensation of Steam in a Vertical Tube in the Presence of Noncondensible Gas," Nuclear Technology, 106, pp. 202 – 214.

6.17. Ghiaasiaan S. M.,. Kamboj B.K. and Abdel-Khalik S.I., 1995, "Two fluid Modeling of Condensation in the Presence of Noncondensible Gas in Two Phase Channel Flows," Nuclear Science and Engineering , 119, pp. 1- 17.

6.18. Nusselt W.A., 1916, "The Surface Condensation of Water Vapor," Ziesrhift Ver Deut. Ing., 60 pp. 541-546 & pp. 569-575.

6.19. Rohsenow W.M., 1956, "Heat Transfer and Temperature Distribution in Laminar Film Condensation," Transactions of the ASME, 78, pp. 1645-1648.

6.20. Rohsenow W.M., Webber J.H. and Ling A.T., 1956, "Effect of Vapor Velocity on Laminar and Turbulent-Film Condensation," Trans. ASME, 78, pp. 1637 – 1643.

6.21. Sparrow E.M. and Lin S. H., 1964, "Condensation Heat Transfer in the Presence of Non-Condensable Gas," Journal of Heat Transfer, 86, p. 430-437.

6.22. Minkowycz W.J. and Sparrow E.M., 1966, "Condensation Heat Transfer in the Presence of Noncondensible Gas, Interfacial Resistance, Superheaing, Variable Properties, and Diffusion," International Journal of Heat and Mass Transfer, 9, pp. 1125 – 1144.

6.23. Vierow K.M., 1990, "Behavior of Steam-Air Systems Condensing in Cocurrent Vertical Downflow," MS Thesis, University of California, Berkeley.

6.24. Ogg D.G, 1991, "Vertical Downflow Condensation Heat Transfer in Gas-Steam Mixtures," MS Thesis, University of California, Berkeley.

6.25. Siddique M., 1990, "The Effects if Non-Condensable Gaases in Condensation Under Forced Convection Conditions," PhD Thesis, MIT.

6.26. Kuhn Y., Schrock V. E. and Peterson P., 1997, "An investigation of condensation from steam-gas mixtures flowing Downward inside a vertical tube," Nuclear Engineering and Design, 177, pp. 53–69.

6.27. Chen S. L. and Ke M. T., 1993, "Forced Convective Film Condensation Inside Vertical Tubes," International Journal of Multiphase Flow 19, pp.1045-1060.

6.28. Kinney R.B., Sparrow E.M., 1970, "Turbulent flow, Heat Transfer, and Mass Transfer in a Tube with Surface Suction," Journal of Heat Transfer, 92, pp. 117-125 (feb.1970)

6.29. Mason E.A. and Monchick L., 1963, "Theory of Transport Properties of Gases," Ninth Symposium (International) on Combustion, New York, Academic Press, pp. 713-724.

6.30. Peterson P. , Schrock V. E. and Kageyama T., 1993, "Diffusion layer theory for turbulent vapor condensation with noncondensible gases," Transactions of the ASME Journal of Heat Transfer, 115, 998 – 1003.

6.31. Yih S.M. and Liu J.L., 1983, "Prediction of Heat Transfer in Turbulent Falling Liquid Films With or Without Interfacial Shear," AIChE 29 no.6, pp. 903 – 909.

6.32. Patankar S.V, 1980,*Numerical Heat Transfer and Fluid Flow*, Taylor and Francis.

6.33. Dobran F. and Thorsen R.S., 1979, "Forced Flow Laminar Filmwise Condensation of a Pure Saturated Vapor in a Vertical Tube," International Journal of Heat and Mass Transfer 23, pp. 161 – 177.

6.34. Goodykoontz J.H and Dorsch D.G., 1966, "Local Heat Transfer coefficients for Condensation of Steam in Vertical Downflow Within a 5/8 inch Diameter tube," NASA Report, TND-3326.

6.35. Siddique M., Golay S. and Kazimi M., 1993, "Local Heat Transfer Coefficients for Forced Convection Condensation of Steam in a Vertical Tube in the Presence of a Non-condensable Gas," Nuclear Technology, 102, pp.386-402.

7. ACCOMPLISHMENTS

Here the accomplishments of the first year are summarized.

- A detailed scaling analysis for the PCCS condenser was performed. The scaling parameters were identified to scale down the prototype condenser design. The effect of the non-condensable in the scaled condenser was discussed and its implication on the scaled test facility was presented.

- An experimental loop was designed with 5.04 cm inch diameter condenser. The design of the condenser tube was based on the scaling analysis. The test section and the loop were instrumented for required parameters.

- There was delay in completing the first year experimental task due to late start of the project. Permission was sought from DOE to extend the first year period 05/01/00 - 04/30/01 to 05/01/00 – 08/31/01, an extension of four months. DOE has granted an extension of four months to complete the first year task. Currently the test loop is being constructed and tested. The first year experimental task will be completed by August 31, 2001.

- A condensation model was developed for forced downflow of steam and non-condensable gas in vertical tube. First the model was tested for pure steam condensation and the predicted heat transfer results were compared with the experimental data. Then the model was tested for condensation in the presence of non-condensable gas, air, and results of the predictions were compared to the published experimental data The agreement was fairly good. Please note that this modeling task falls in second year period. Since the first year task on experiments has been extended to be performed by four months, this period of work is taken care by the modeling task, which ultimately will be refined and studied in detail in second year.